AIAA Journal

RUSSIAN SUPPLEMENT

Igor Jurkevich, Editor

Some Results Obtained with the 22-Meter Radio Telescope

A E Salomonovich

I Introduction

THE first radio astronomy observations were conducted with relatively small radio telescopes The need for instruments of the largest possible dimensions did not become apparent until the early 1950's At meter wavelengths, where the problem of improving the resolving power is more important than that of increasing the effective area of the telescope, dimensions are usually increased by building multiple-unit interference systems of various kinds At decimeter and centimeter wavelengths the usual method of increasing the effective area—which is the primary requirement at these wavelengths—is to change over to larger and larger reflector antennas

When the large reflecting radio telescope built by the Lebedev Physical Institute was designed,* it was decided to try to obtain the maximum possible precision and rigidity of the working surface, so that observations could be conducted at wavelengths as short as 1 cm The choice of the diameter of the aperture of a parabolic reflector is limited by the permissible deformations Preliminary calculations showed that it would be possible to get a reflector with a diameter of 15–20 m, which would provide a beam width of the order of 2 min of arc at the shortest wavelength used The research program for which the telescope was to be used was predicated on this resolving power

Translated from Trudy Fizicheskogo Instituta im Lebedeva (Transactions of the Lebedev Physical Institute, USSR Academy of Sciences) 27, 42–83 (1962) Translated by Jean Findlay, Green Bank, West Virginia Reviewed by Edward F McClain, Radio Astronomy Branch, U S Naval Research Laboratory, Washington, D C

* At the initiative of S E Khaikin

II Research Program

One of the advantages offered by large reflecting radio telescopes is their versatility Thus a fairly broad range of problems can be solved with the 22-m telescope

1 Physical Conditions on the Moon and the Planets of the Solar System

The opportunity of observing the radiation emitted by the moon and planets at various wavelengths in the centimeter range enables observers, by studying the spectrum of the radiation and its variation with the phases of the moon and such planets as Venus and Mercury, to form an idea of physical conditions in the surface layers and atmospheres of the planets (temperature, density, composition, etc) High resolution in a radio telescope makes it possible to measure the distribution of radio brightness across the moon's disk and to try to identify differences in the properties of the various areas—the seas and continents—on its surface Ob-

servation of sporadic radiation from Jupiter and possibly other planets is of special interest, as are attempts to detect water vapor in the atmosphere of Venus and to determine the sense and period of its rotation

This type of research is particularly important in that the moon and the nearest planets will probably be our first goals when interplanetary flight begins

2 The Physical Nature of the Discrete Radio Sources

Radiation from various galactic and extragalactic discrete sources—the latter being radio nebulae—originally detected at meter wavelengths, is generally diverse in nature The determining factor in learning the nature of radiation from various sources is a knowledge of the frequency dependence of the received power and its polarization Thus the investigation of sources at decimeter, as well as centimeter and millimeter, wavelengths is of considerable interest The high resolving power of the 22-m telescope often makes it possible to determine the angular dimensions of the source as well A related task of no less importance is the investigation of the brightness distribution of galactic radiation at centimeter and decimeter wavelengths, and particularly the polarization of such radiation

3 Physical Conditions in the Lower Layers of the Sun's Atmosphere and the Nature of Localized Radio Sources on the Sun

The high resolving power of the 22-m telescope at ~1 cm wavelengths makes it possible to investigate the distribution of radio brightness on the sun's disk, to obtain a radio picture of the sun, and to detect and study the behavior of the active areas on its disk in the short-wave portion of the centimeter range, especially their state of polarization This enables observers to make comparisons with optical data and with data obtained at longer wavelengths and thus to draw inferences as to the nature of the active areas

Spectral studies of the bursts of radiation at centimeter wavelengths, and particularly the location of the sources of this radiation in the active areas, throw light on the nature of active processes on the sun that are directly related to geophysical phenomena and the origin of solar cosmic rays

4 Monochromatic Radiation and Selective Absorption in the Galaxy and Metagalaxy, and Selective Absorption in the Sun's Atmosphere

Unlike the radiation from most radio astronomy sources, which has a continuous spectrum, the radiation from neutral hydrogen—the main constituent of the interstellar material—and the radiation predicted by theory from a number of other molecules occurs at precise frequencies determined by the energy levels of the quantum states involved The presence of monochromatic radiation, and the corresponding absorption, have opened up new possibilities for studying the universe The narrow beam width of the 22-m telescope at a wavelength of 21 cm (~40 min of arc) makes it possible to resolve comparatively small areas of the sky at the hydrogen-line frequency, as well as to observe the effect of selective absorption in the interstellar hydrogen of radiation from discrete sources in order to study the distances to such sources The theoretically predicted lines of selective absorption in the radiation of the sun's atmosphere at centimeter wavelengths, given adequate sensitivity of the equipment used, can also be studied with the 22-m telescope

5 The Radiation, Absorption, and Density Fluctuation of the Earth's Atmosphere

It is known that the Earth's atmosphere emits considerable radiation at centimeter and millimeter wavelengths The investigation of this radiation in terms of weather conditions and height above the horizon, as well as time variations in the radiation, provides valuable information on the state of the atmosphere Experiments can also be set up to study the polarization of atmospheric radiation in order to clarify the relative parts played by absorption and scattering in attenuating radio waves propagated in the atmosphere

III Testing the Parameters of the 22-m Antenna

The research program outlined in the foregoing was drawn up while the telescope was still in the design stage and obviously could not be planned in detail at that time The chief obstacle was uncertainty as to how close the electrical parameters of the antenna would come to the standards required for the performance of certain parts of the program Thus the first task to be undertaken after the installation of the telescope had been completed and the instrument adjusted was to study its electrical parameters Before this could be done the electrical axis of the antenna had to be aligned The measurements of the parameters of the telescope were made while it was being used for certain other programs, the main results of which have been published in Refs 1–3

These measurements of parameters involved some fairly serious difficulties For a reflector aperture of 22-m diam, measurements of the antenna patterns should be made at great distances at 3-cm wavelengths and at even greater distances at 0 8-cm wavelength The Fraunhofer region at 3 2- and 0 8-cm wavelengths begins at distances of ~30 and ~120 km, respectively Under these conditions the usual methods of making antenna measurements are of little or no use, so that special procedures had to be devised

There were two systems of measurement. In the first, extraterrestrial discrete radio sources were observed, and in the second, a terrestrial generator inside the Fresnel region was used

The technique of measurement and results obtained at 9 6-, 3 2-, 0 8-, and 0 4-cm wavelengths are described in the following

1 Measurements Using Discrete Sources

The advantages of this method are obvious: Extraterrestrial discrete radio sources are so far from the antenna being studied that they always lie in the Fraunhofer region Their coordinates are very precisely known at any given moment But at the same time, use of the method creates new problems due to the finite angular size and the variation in spectral characteristics of the sources of extraterrestrial radiation The use of extended sources, such as the sun and the moon (with the exception of one variation of the method, to be discussed next) for measuring the antenna pattern was restricted by the small beam width of the 22-m telescope This fact ruled out altogether the use of certain extended sources, the angular dimensions of which have not yet been determined with sufficient accuracy

In addition, the low radiation fluxes available even at centimeter wavelengths and even for the strongest sources made it difficult to measure antenna characteristics at the shorter wavelengths of 0 8 and 0 4 cm For this reason we had greater success in using discrete sources to measure antenna characteristics at the 9 6- and 3 2-cm wavelengths

At these wavelengths we used strong discrete sources having rather small angular dimensions: Cassiopeia A, Cygnus A, Taurus A, and Virgo A at 9 6-cm wavelength and Taurus A at 3 2-cm wavelength

Before measuring the antenna parameters we had to align the electrical axis of the antenna with the axis of the optical telescope and with the zeros on the graduated dials, and to position the phase center of the feed at the focus of the parabolic reflector This was done by selecting a position of the

Table 1

Source of radiation	α1960	δ1960
Cassiopeia A	23 hr 21 min 33 sec	58 35′ 3
Cygnus A	19 58 06	40 36 6
Virgo A	12 28 49	12 36 7
Taurus A	5 32 15	22 00

feed (which was a conical horn) on the axis of the paraboloid† for which the signal received when Cassiopeia A was in transit across the stationary antenna pattern was a maximum Since the solid angle of the source is considerably less than the effective solid angle of the antenna pattern, the best position of the feed corresponds to the maximum over-all gain of the antenna

The measurements made at 9 6 cm wavelength showed that when the feed is moved 0 1λ along the axis of the paraboloid the antenna gain decreases by not more than 2 5% (with a relative accuracy of better than 1%)

The electrical axis of the antenna was aligned by comparing the calculated transit times of the sources Cassiopeia A, Cygnus A, and Virgo A across the stationary antenna pattern with the times of the maxima in the recorded transit curves The calculated positions were set by using the verniers on the azimuth and elevation circles The zero references of these verniers coincide to within 10 sec of arc with the axis of the optical telescope The coordinates of the sources used were those in Ref 4 or were taken from the NGC catalog in Table 1

Since we knew the rate of movement of the source on the celestial sphere $v = 15 \cos \delta$('/min), we could convert the time intervals to angular intervals For example, the electrical and optical axes coincided in azimuth, according to the measurements made at 9 6-cm wavelength, to within $\pm$0 25 min of arc In elevation, the electrical axis was systematically 2 min of arc above the optical axis This was allowed for in future measurements At 3 2-cm wavelength the divergence of the axes with the feed in a central position was of the same order

The antenna patterns were obtained by recording the transit across the stationary antenna of the sources Cassiopeia A and Cygnus A at 9 6-cm wavelength and Cassiopeia A and Taurus A at 3 2-cm wavelength The principal planes of the feed were oriented in such a way that the transit of the source at culmination produced a pattern for either of the principal cross sections (E plane or H plane) To do this the feed was rotated $\pi/2$ about its axis With a fixed orientation of the feed it was also possible to obtain patterns in the E and H planes by recording the transit of the nonsetting source Cassiopeia A not only at the upper and lower culminations but also at the reversal points of its trajectory (for example for the two hours before or after upper culmination) At intermediate points of the daily trajectory of the sources "diagonal sections" of the antenna pattern were obtained

Within the limits of errors in measurement, the antenna pattern showed predominantly circular symmetry This was a result of the special choice of size of the aperture of the conical horn ($d \backsimeq \lambda$) Calculations showed that a feed of these dimensions with an angular aperture of about $2\psi = 120°$ would give equal excitation of the reflector in the principal planes Figure 1 is a sample of the patterns obtained on reducing the records of the transit of Cassiopeia A at 9 6-cm wavelength The average of the 27 measurements of the 3 db beam width was 19′ 0 $\pm$ 0′ 5 at 9 6-cm wavelength ‡

† The image of the center of the feed aperture was superposed on the cross wires of the telescope located at the apex of the paraboloid

‡ The theoretical 3 db beam width with optimum illumination should be 18′ 3 in the H plane and 19 6 in the E plane (This footnote is not referred to in the body of the text, but the asterisk has been inserted where it is believed logically to be long—Translator)

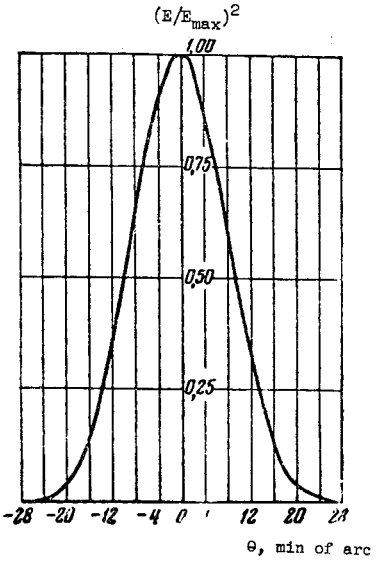

Fig 1 Antenna pattern of radio telescope at 9 6-cm wavelength

The side lobes did not exceed -20 db At 3 2-cm wavelength Cassiopeia A was not used for determining the antenna pattern, because of uncertainty as to the size and shape of the curve of its brightness distribution The beam width could be determined from the transit of Taurus A, the angular size of which was taken, according to the data of Apushkinskii and Pariiskii,[5] as 3′ 4 The records of the transit of this source showed the antenna pattern to be symmetrical, its width being 6′ 4 $\pm$ 0′ 2 in both planes This agrees within the errors of measurement with the result obtained by the second method, described next, and with the value obtained theoretically Here, too, the side lobes do not exceed -20 db In reducing the transit records we used the final source dimensions given in Ref 6; the brightness distribution of the source and the shape of the main beam of the antenna pattern were taken to be approximately Gaussian The sensitivity of the radiometers used was rather high, so that small (τ = 5 sec) time constants could be used Thus the corrections for the commensurability of the transit times of the sources through the stationary antenna beam and the radiometer time constant were small, and distortions of the curve could be ignored [7]

At 0 8 cm wavelength, and subsequently at 0 4-cm wavelength as well, the antenna pattern was also obtained in a few experiments using terrestrial sources of radiation In 1959 we obtained at 0 8-cm wavelength records of the transit of localized sources of radiation near active areas on the solar disk, which indicated that the width of the antenna pattern did not exceed 2 min of arc (Fig 2) Similar results were obtained from the records of the transit of Venus through the beam At 0 4-cm wavelength an estimate of the beam width was also made from observations of the radiation from Venus

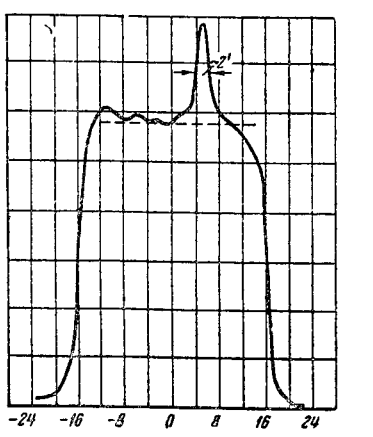

Fig 2 Drift curve of the sun's disk across pattern of radio telescope at 0 8-cm wavelength

and was close to 1′ 6 Similar measurements of the patterns at 0 8- and 0 4-cm wavelengths are described next

The antenna gain at 9 6- and 3 2-cm wavelengths was determined by measuring the intensity of discrete radio sources The intensity of radiation from radio astronomy sources can of course be defined by the flux density p dependent on the brightness of the source I in the relationship

$$p = \int_{4\pi} I(\Omega)d\Omega$$

The brightness I is expressed by the brightness temperature of the source T_b—the temperature of an ideal black body having, at a given frequency and in a given direction, the same brightness as the source under study In the radio frequency region for the ideal black body $T_b = (\lambda^2/2k)I$, where k is the Boltzmann constant Therefore

$$p = \frac{2k}{\lambda^2}\int_{4\pi} T_b(\Omega)d\Omega$$

The increment in the temperature T_A of an antenna directed at the source is a quantity that is directly measured in radio astronomy For T_A the relationship

$$T_A = \frac{\int_{4\pi} T_b(\Omega)F(\Omega)d\Omega}{\int_{4\pi} F(\Omega)d\Omega}$$

applies, where $F(\Omega)$ is the power response pattern of the antenna When the solid angle of the source Ω (measured, for example, at the half-brightness points) is much smaller than the solid angle of the antenna pattern Ω_A, the relationship

$$T_A = \frac{\int_{4\pi} T_b(\Omega)d\Omega}{\int_{4\pi} Fd\Omega} = \frac{1}{4\pi}G\int_{4\pi} T_b(\Omega)d\Omega$$

is correct, in which $G = 4\pi/\int_{4\pi} F(\Omega)d\Omega$ is the antenna gain Hence when $\Omega \ll \Omega_A$ we have

$$p = \frac{2k}{\lambda^2}\frac{4\pi T_A}{G} = \frac{2k}{A}T_A$$

where $A = (\lambda^2/4\pi)G$ is the effective area of the antenna In the case when Ω_s is commensurate with Ω_A, we have the relationship

$$T_A = \frac{\int_{4\pi} T_b(\Omega)d\Omega}{g\int_{4\pi} F(\Omega)d\Omega} = \frac{1}{4\pi g}G\int_{4\pi} T_b(\Omega)d\Omega$$

where g is a coefficient allowing for commensurability of the angular dimensions of the source and the antenna pattern In the particular case of a Gaussian approximation for the brightness distribution of the source and the antenna pattern[8]

$$g = 1 + (\varphi/\varphi_A)^2$$

where φ and φ_A are the angular dimensions of a symmetrical source and pattern at the 3 db points

When Ω_s is commensurate with Ω_A we have

$$p = (2k/A)gT_A$$

Measurements of T_A at 9 6-cm wavelength were made using a GN-2 gas-discharge-tube noise generator loosely coupled to the waveguide At 3 2-cm wavelength similar measurements were made using a cooled thermal load[7] The measurements were intended to determine the effective area of the antenna A, so that, in addition to T_A, the flux p and the size of the source were needed to find the value of the gain g The choice as reference source of the fairly strong discrete source Taurus A, the flux density of which changes slowly with frequency, reduced the errors due to frequency interpolation Analysis of published data on measurements of this source[1] showed that the most probable value of the flux at 9 6-cm wavelength was $p = 7\,9 \times 10^{-24}$ w/m²/hertz, and the 3 db angular size was $\varphi = 4'$

A comparison of these data with the average value obtained on the radio telescope for the antenna temperature of the source, $T_A = 52\,3 \pm 0\,5°$, gives a value for the effective area of the antenna at 9 6 cm wavelength of $A = 190 \pm 30$ m² The errors made were due chiefly to uncertainties in the value of the flux of Taurus A

The corresponding antenna gain is $G = 2\,6 \times 10^5 \pm 15\%$

The gain as determined by integrating the antenna pattern over the volume of the main beam was $G_0 = 3\,8 \times 10^5$ From this we determined the stray factor β, describing the radiation in the side and back lobes, which decreases the effective area of the antenna By definition $\beta = (G_0 - G)/G_0 = 0\,32$

A comparison of A and $A_{g\ om}$, where $A_{g\ om}$ is the area of the aperture of the paraboloid, gives an aperture efficiency of 0 58 Here $A_{g\ om} = 0\,85(\pi D^2/4)$, where D is the diameter of the aperture, since approximately 15% of the area of the aperture is shaded by the tetrapod feed support

A similar method was used to determine the effective area of the antenna at 3 2-cm wavelength The flux of the reference source Taurus A was obtained by extrapolating to 3 2 cm the spectrum measured at longer wavelengths; it was $6\,0 \times 10^{-24}$ w/m²/hertz

In making measurements of the antenna temperature T_A at 3 2 cm wavelength allowances had to be made for the linearly polarized component of the radiation of the source Measurements made at a different time of day and consequently at different angles of parallax γ of the extended source gave different values for T_A, which confirmed the presence, detected earlier,[9] of polarization of the source Taking account of the degree of polarization (7%) and the direction of maximum polarization ($\varphi = 149°$) obtained in Ref 9, we determined the average antenna temperature, $T_A = 40°$K, which gave a value for the effective area of the antenna of $A = 185 \pm 30$ m² This corresponds to an aperture efficiency of an unshaded surface of 0 57 The corresponding antenna gain was $G = 2\,26 \times 10^6 \pm 15\%$

2 Measurements with a Transmitter in the Fresnel Region

At 0 8-cm wavelength it is at present virtually impossible to make measurements by the method described in the foregoing, since the angular dimensions of strong discrete sources are larger than the pattern to be measured and the flux of the sources is too weak for measurements to be reliable A second method, suggested by N A Esepkina,[10] was therefore used to measure the antenna pattern It was essentially as follows: On the aperture of the paraboloid to be studied phase corrections were produced, compensating for the phase errors caused by the finite distance to the transmitter in the Fresnel and not in the Fraunhofer region This compensation was achieved by moving the feed out a calculated distance b from the focus along the axis of the paraboloid

If $b \ll f$, where f is the focal length, then the departures from phase equality over the aperture resulting from moving the feed out can be represented in the form

$$\psi(x) \approx kb[1 - (x^2/4f^2)]/[1 + (x^2/4f^2)]$$

where x is the distance of a point on the aperture from the axis of the paraboloid On the other hand, the phase departure due to the finite distance to the transmitter is

$$\varphi(x) \approx kx^2/2R$$

where R is the distance to the transmitter

The condition for compensation is $\varphi(x) + \psi(x) = kb$ As a function of the parameter h/f, where $h = D^2/(16f)$ is the

depth of the paraboloid, and depending on the form of the excitation, the function $\psi(x)$ can be approximated by one of the expressions

$$\psi_1(x) \approx -\frac{kbx^2}{2f^2} \qquad \psi_2(x) \approx -\frac{kbx^2}{2f^2}\,\frac{2}{1 + D^2/16f}$$

where the constant phase shift kb for the entire aperture is ignored For paraboloids with a ratio $h/f > 0\,2$, of which the 22-m paraboloid is one ($D = 22$ m; $f = 9\,525$ m), the best approximation is the function $\psi_2(x)$

For measurement it was convenient to locate the transmitter at a survey point distant $R = 3250$ m from the radio telescope in an almost exactly southerly direction (The distance was determined by triangulation) From $\varphi(x) + \psi(x) = 0$, we obtain $b = 37$ mm Here the ratio $b/f = 0\,004$, which satisfies the condition of applicability of the method The transmitter used was a klystron generator with an attenuator and waveguide, radiating through a small horn 6 m above the earth's surface

The antenna patterns were obtained by slowly rotating the radio telescope in azimuth and reading the position of the electric axis on the circle The best position of the axis was found by adjusting in elevation

To reduce errors due to variations of the transmitter frequency relative to the local oscillator, many transits were observed at a controlled frequency The patterns were obtained both for the calculated position of the feed (9525 + 37 mm) and with deviations from this position of 5, 10, and 15 mm With the feed—which was the open end of a circular waveguide 6 mm in diameter—in the position that gave the greatest sharpness of the antenna pattern and the lowest level for the side lobes, the patterns obtained in this way indicated a focus which agreed to an accuracy of ±5 mm with the theoretical focus of the paraboloid determined by the method described in Ref 11

Figure 3 shows a typical H-plane pattern obtained at 0 8-cm wavelength by azimuth transit with the E vector vertical The 3 db beam width in the H plane obtained by averaging a number of records at the best feed position was $1'\,7 \pm 0'\,1$ (cf Fig 3) The beam width in the E plane obtained by elevation transits, which were considerably affected by the ground, was $2'\,1 \pm 0'\,1$ The theoretical beam width with optimum excitation should be $1'\,6$ in the H plane and $1'\,7$ in the E plane The level of the first side lobe was −12 2 db The wide-rangle lobes could be clearly seen when the sensitivity of the receiver was increased, and their size decreased monotonically with their angle from the main beam

The antenna gain at 0 8-cm wavelength was roughly estimated from the measured antenna pattern by the usual formula:

$$G = 4\pi/\int_{4\pi} F(\Omega)d\Omega$$

where F is the power response pattern of the antenna

Graphic integration was carried out over the main beam and the side lobes The calculations gave

$$G_{01} = (3.4 \pm 0\,3)\ 10^7$$

If the integration is taken only over the main beam $G_0 = (4\,2 \pm 0\,4) \times 10^7$ If the stray factor is taken as $\beta \leqslant 0\,50$, then

$$G \geqslant (1\,7 \pm 0\,2)\ 10^7$$

which corresponds to an effective area of $A \geqslant 116 \pm 25$ m²

Measurements of the antenna pattern by this method were made at 3 2-cm wavelength as well and gave results which agreed within the errors of measurement with those obtained by the discrete-source method Measurement of the pattern at the wavelength of 0 8 cm obtained with a portable

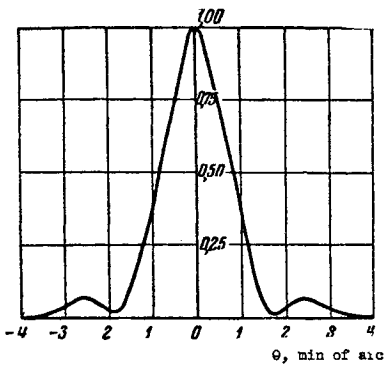

Fig 3 Antenna pattern of radio telescope at 0 8-cm wavelength

transmitter were repeated at the beginning of 1960 and in the autumn of 1961 The results obtained were the same

Increasing the sensitivity of the receiver in 1961 made it possible to estimate more precisely the effective area A at 0 8-cm wavelength by measuring the radiation of Jupiter [12] It was found that $A = 108 \pm 20$ m², which is close to the foregoing estimate The value[1] $A = 150$ m² is obtained when $\beta = 0\,35$

In March 1961 further measurements of the antenna parameters were made at 0 4-cm wavelength As these measurements were made over a limited time it was impossible to choose the best feed position in advance As a result, the antenna parameters obtained from the measurements and used in reducing observations[3] made during this period were probably not the best possible ones Since the method of obtaining these parameters is of interest, it will be described in brief

The sun, moon, and Venus were used as sources of radiation

From many records of the transit of Venus across the antenna pattern the 3 db beam width was found to be $1'\,6$ To find the effective area of the antenna, known data on the brightness temperature of the moon were used, and observations were made with the radio telescope of transits when the center of the sun passed through the antenna beam

The brightness temperature of the moon, T_{bm}, which can be taken with sufficient accuracy to be constant within the limits of the solid angle subtended by the moon Ω_m, is related to the antenna temperature of the moon by the obvious relationship

$$T_{bm} = \frac{\lambda^2}{A}\,\frac{T_{Am}}{\int_{\Omega M} F(\Omega)d\Omega}$$

Hence the effective area of the antenna can be found if T_{Am} is measured, T_{bm} is known, and the integral in the denominator is calculated For this we must know the form of the antenna pattern within the limits of the solid angle Ω_m The approximate form of $E(\Omega)$ was obtained as follows: On the basis of the beam width known from the transit records of Venus, an equivalent pattern was constructed so that the central transit of the solar disk across this pattern gave a curve which coincided with the observed curve The model was a Gaussian curve with a 3 db width of $1'\,6$ and "wings" chosen to satisfy the requirement referred to in the foregoing On the basis of the value of the brightness temperature of the moon in the phases in which T_{Am} was measured, which is known with an accuracy of 10%, the effective area of the antenna at 0 4-cm wavelength was determined and the stray factor of the antenna outside the main beam was found to be 0 7

IV Review of Results of Observations of the Sun, Moon, and Planets

The observations made with the 22-m radio telescope during the two years it has been in operation fall under the first

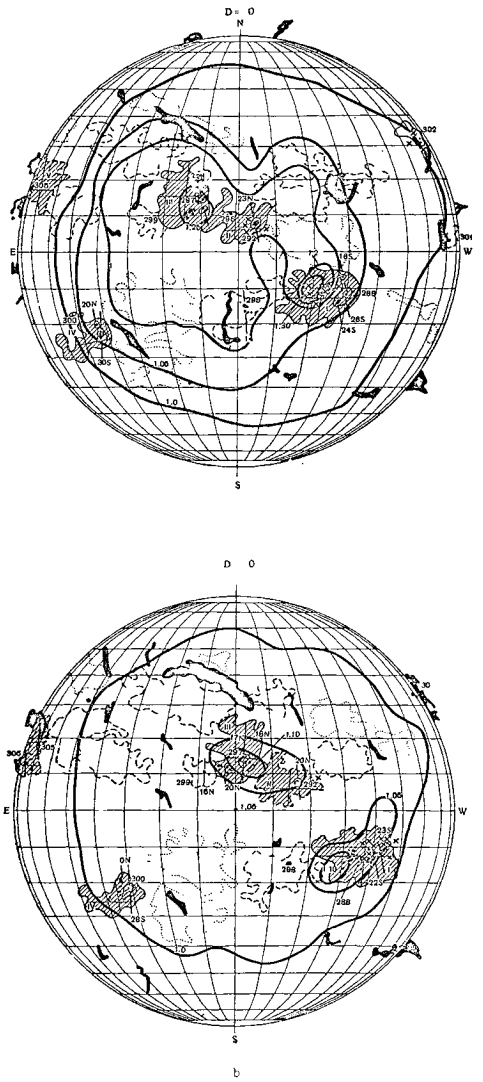

Fig 4 Radio pictures of the sun at 0 8-cm wavelength made June 6 (a) and June 7 (b), 1959 Solid lines are radio isophotes plotted on heliogram

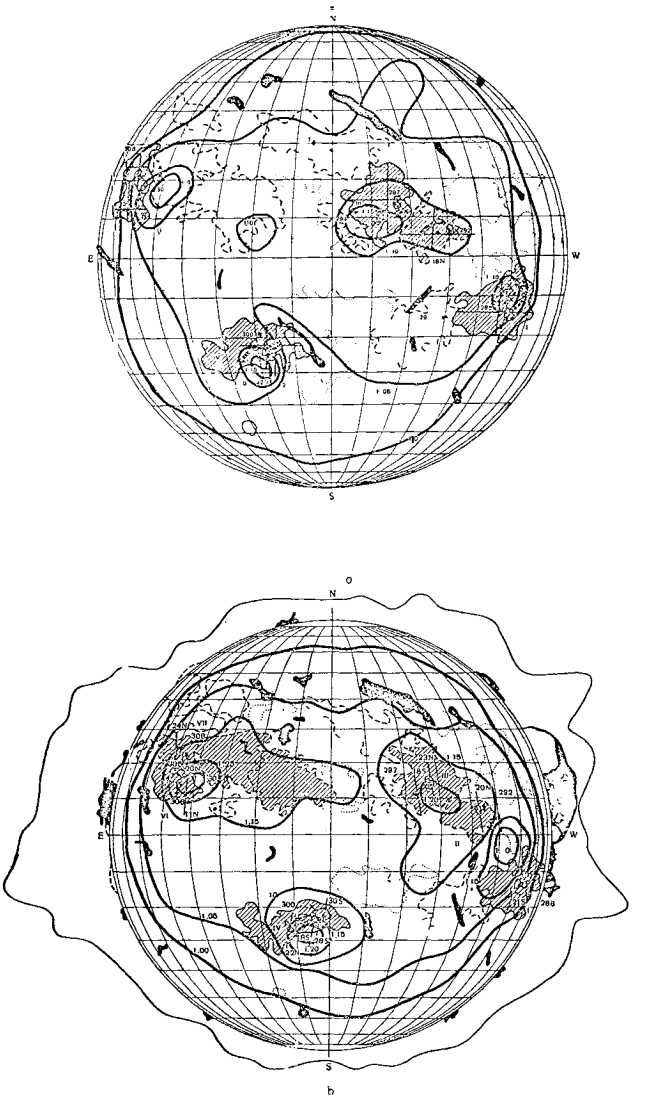

Fig 5 Radio pictures of the sun at 0 8-cm wavelength made June 8 (a) and June 9 (b), 1959 Notation as in Fig 4

three headings in Sec II The chief results obtained in studying discrete sources of radiation have been published by Kuz'min [13] We shall refer briefly to the results of observations of the radiation of the sun, the moon, and the planets

1 The Sun

Observations of solar radiation at 0 8-cm wavelength, made at the Physical Institute since 1954 using a radio telescope with a parabolic reflector 2 m in diameter, have revealed not only the components of the radiation of the quiet sun but also a brightness temperature distribution over the disk which agrees with the two-component model of the solar chromosphere,[14] and the presence of a slowly varying component,[15] the strength of which shows satisfactory correlation with the total sun-spot area (coefficient of correlation 0 4 ± 0 04) The mean brightness temperature of the disk, averaged for a long period close to maximum solar activity (1957–1958), was slightly higher than 8000°K The minimum brightness temperature obtained by extrapolation to a total spot area equal to zero was close to 7000°K

But the relatively low resolution of the telescope made it impossible to determine the detailed distribution of brightness temperature over the solar disk With the 22-m telescope, measurements of solar radiation have been made mostly at 0 8-cm wavelength, but also at 2 and 3 2 cm The first records of a two-dimensional distribution of radiation made at 0 8-cm wavelength beginning in May 1959 showed the presence of local areas that were brighter than the level corresponding to radiation from the quiet sun Regular observations made in June 1959 produced day-by-day radio pictures of the sun and revealed a connection between the characteristics of these radio pictures and the behavior of the active areas occurring on the disk on the date of observation Figures 4 and 5§ show typical radio images—two-dimensional distributions of the antenna temperature of the sun—with the heliograms published in the Solar Data Bulletin superimposed Most of the radio pictures were constructed from records of the transit of the solar disk across the antenna pattern of the radio telescope in conditions when the sun was unobscured, so that tracking in one of the coordinates was done visually Some of the radio pictures were obtained from "blind" records For this reason some of them—that of June 16, 1959, for example—are lacking in detail

The radio isophotes were plotted in relative units, the unit taken being the level of the quiet sun No correction was made for antenna pattern smoothing Analysis of the records showed the presence of areas of enhanced radio brightness These areas are located above large groups of spots (spot area $S_p \geqslant 100$) and apparently consist of radiation

§ The original paper contains seven additional figures of this nature—Editor

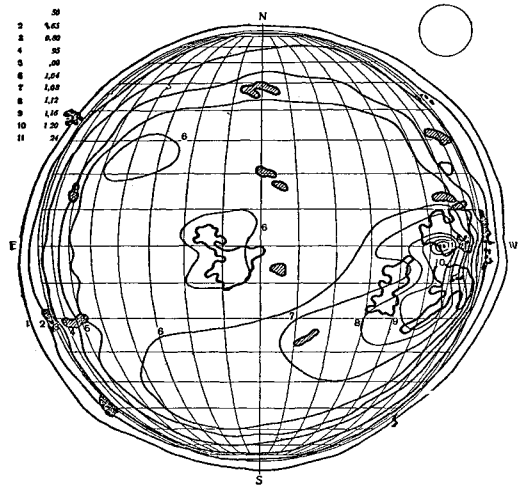

Fig 6 Radio picture of the sun at 2-cm wavelength made February 14, 1961 Figures at left represent antenna temperature in proportion to temperature of the quiet sun; circle to right shows size of antenna pattern

from coronal condensations, chiefly the lower parts of the condensations The angular dimensions of the central part of the most active areas, where $S_\nu \geq 300$–500, are approximately 1–2 min of arc Enhanced radiation was also observed from more extended areas (4–5 min of arc) having dimensions close to those of the calcium flocculi ("pedestals") The increase in brightness temperature of the bright areas over the level of the quiet sun reaches (2 5–6)10^3°K in the central nuclei The level of the pedestals often does not exceed 5–10% of the quiet-sun level The process of development of some ten active areas was observed The dimensions of the extended pedestals showed excellent correlation with those of the corresponding flocculi Cases were also observed in which the areas of enhanced radiation were related not to groups of spots but only to the presence of a calcium floccula (fields of faculas) Such cases occurred in the period June 20–23, 1959, as observed at 0 8-cm wavelength, and in February 1961 as noted from observations of the radio brightness distribution of the sun at 2-cm wavelength Figure 6¶ shows an example of distributions observed by B Ya Losovski on February 14–16 In this period—measurements were made from February 12 to 18—in addition to groups of spots flocculi were also observed, which gradually moved across the disk from the eastern limb ($\lambda = -40°$, $\varphi = -50°$) to the center These flocculi were related to relatively weak areas of increased brightness It is interesting that there were no spots inside the flocculi Apparently the areas of enhanced radiation at 1–2-cm wavelengths can come into being not only in the presence of groups of spots but in other ways as well, which explains the relatively lower correlation with the total spot area mentioned previously As a rule, localized sources at 0 8-cm wavelength appear somewhat later and disappear somewhat sooner than the corresponding groups of spots Some correlation is evident between the total area of a given group of spots and the maximum brightness temperature of the corresponding localized source

On certain days simultaneous measurements were made at 0 8- and 3 2-cm wavelengths, and also at about 2-cm wavelength These measurements showed that the flux densities of localized sources measured at the foregoing wavelengths were closely similar: this apparently indicates the thermal origin of radiation from these sources, which at 0 8- and 3 2-cm wavelengths are optically thin

Measurements were also made of the polarization of radiation from localized sources, confirming the presence of circular polarization at 3 2- and 2-cm wavelength The presence was also noted of circular polarization of radiation from active areas at 0 8-cm wavelength The results of these last measurements, prepared by U V Khangil'din, are being made ready for publication

Bursts of radiation at 0 8-cm wavelength were also definitely located on the solar disk in two cases [16] The beginning of the bursts coincided with chromospheric flares An estimate of the angular dimensions showed them to be 1–2 min of arc The maximum brightness temperatures of the bursts seem to have reached 10^4–10^6 °K Further investigation of the spectrum, polarization, and localization of bursts will reveal their physical nature

2 Lunar Thermal Radiation

The electromagnetic radiation of the moon in the radio-wave range is known to provide evidence as to the temperature and certain physical characteristics of the surface layer emitting the radiation

Radio telescopes of high resolving power at millimeter and centimeter wavelengths make it possible to measure not only the average values of brightness temperatures but also the distribution of these temperatures over the disk as a function of the phase of the moon

To determine the characteristics of various sections of the lunar surface, we must have, in addition to radio observational data, the distribution of the surface temperature, obtained from radiometric measurements in the infrared part of the spectrum Since hardly any such data are available, we must make use of models constructed in part on the assumption that the moon's surface is homogeneous However, measurements made with a pencil-beam radio telescope, such as the 22-m telescope at centimeter wavelengths, now make it possible to obtain directly the way in which the emissivity and the surface temperature vary over the moon's disk [17] A knowledge of these functions is a prerequisite for using the measurements of the brightness temperature distribution to obtain the ratio between the penetration depths of an electromagnetic wave and a thermal wave of the same periodic variations, which depends on the thermal and electromagnetic characteristics of the surface layer material

The observations made with the 22-m telescope in 1959–1960 at a series of centimeter wavelengths (0 8,[18] 2,[19] 3 2,[20] and 9 6 cm[21]) enabled observers, following the theory of variations in brightness temperature with the nature of the material,[22] to obtain new data on the physical conditions in the moon's surface layer At 0 8, 2, and 3 2 cm, two-dimensional distributions of the brightness temperature (radio pictures) were obtained

For example, Fig 7 is a typical record, and Fig 8** shows a typical radio picture obtained at 0 8 cm after correction for antenna smoothing

The area of maximum radio brightness at 0 8–3 2 cm wavelengths shifts regularly along the lunar equator following the subsolar point In addition, there is a constant attenuation of brightness from the equator to the poles, caused by the decrease of the surface temperature with the latitude ψ The divergence of the isophotes from axial symmetry which is evident in many of the radio pictures may be due to differences in the properties of the various areas (seas and continents), but this needs confirmation

The phase dependence of the radio brightness distribution shows that during the lunar month the layers emitting radiation at ~1–3 cm wavelengths undergo considerable temperature variation, unlike the lower layers, which radiate at longer wavelengths This dependence results in a periodic fluctuation in brightness temperature at the center of the disk T The fluctuations increase as the wavelength becomes shorter At 9 6 cm the fluctuations do not exceed 2% T_0, the average value of T, was determined with an accuracy

¶ Two similar figures present in the original paper have been eliminated from the translation—Editor

** Three additional figures are given in the original paper—Editor

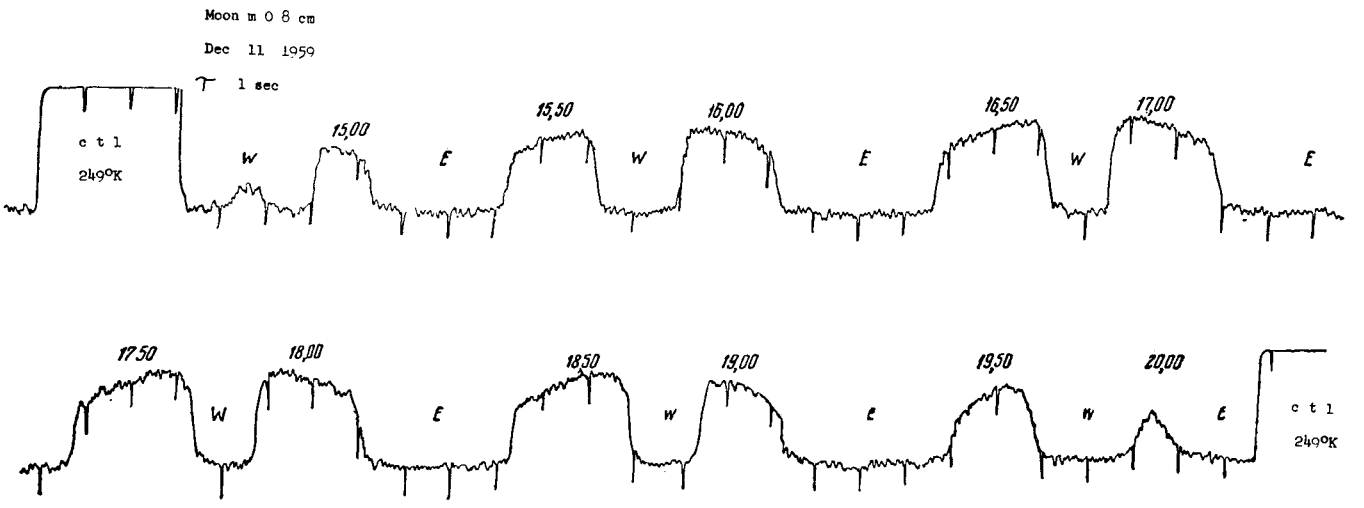

Fig 7 Typical drift curve of the moon's disk at 0 8-cm wavelength Figures above record show optical telescope alignment; "c t l " is the record of the radiation from the cooled thermal load

of ±15% and differed somewhat for the measurements at different wavelengths: At 0 8, 2 0, 3 2, and 9 6 cm, T_0 was equal to 210, 190, 223, and 230°K, respectively More careful calculation of the antenna parameters of the telescope decreases this difference and gives the value $T_0 = 230$°K Analysis of the results of measurement at 0 8- and 2 0-cm wavelengths by a method developed some time ago[17] shows that the effective dielectric constant of the surface layer appears not to exceed 1 5–2, and the latitude distribution of the surface temperature is satisfactorily given by the function $\sqrt{\cos\psi}$ In more recent reductions of results, more precise values for surface temperatures in the center of the disk were used for the lunar noon (407°K) and the lunar midnight (125°K), measured in the infrared area

Table 2 gives the ratios between the amplitude of the first harmonic of brightness temperature in the center of the disk $T \div$ and the average temperature T_0, and between the depths of penetration of a radio wave and a thermal wave of the first harmonic δ, computed in accordance with the theory of V S Troitski [22] It also shows the values of the temperature lag ξ relative to the optical phase The values obtained with the 22-m telescope are compared with the values published earlier at 1 25-,[23] 1 63-,[24] and 20 5-cm wavelength [25]

For $\lambda > 1$ cm the value of $\delta/\lambda \approx 2$ At 0 8-cm wavelength $\delta/\lambda \approx 2\,5$, which somewhat exceeds the value given although it is close to it The constancy of the radio δ/λ shows that there is approximate constancy of the properties of the layer radiating at 1–3 cm

In Jaeger's paper[26] the question of the possible structure of the surface layer of the moon is considered theoretically For comparison with this paper the average values of brightness temperatures in the center of the disk T_0 obtained at 0 8–3 2-cm wavelengths were reduced to the more reliable values, 230°K, obtained at 9 6 cm The parameter $C = \sqrt{\pi/\delta}$ given in Jaeger's paper was reduced for 0 8-, 2-, and 3 2-cm wavelengths in Table 2 The curves of variation in the brightness temperature in the center of the disk with the phases of the moon, calculated by Jaeger, were corrected to take account of the more precise surface temperature values given in the foregoing [27]

On the basis of these data theoretical curves were constructed to show the behavior of T as a function of C corresponding to 0 8-, 2 0-, and 3 2-cm wavelengths, and to such values of the parameter $(k\rho c)^{-1/2}$ which satisfy the variation in surface temperature at the time of a lunar eclipse (Fig 9) observed by Pettit and Nicholson [28] The behavior of the variation of temperature T_c with phase which we observed satisfactorily agrees with the curves constructed for $(k\rho c)^{-1/2} = 400$–1000 Within the limits of precision of measurement it is difficult to give preference to any one of these curves The data obtained with the 22-m telescope attest more reliably than the earlier ones to the correctness of a single layer model of the surface of the moon Here we must take $(k\rho c)^{-1/2} \leqslant 10^3$ This speaks in favor of the presence of an extremely porous and loose material This is corroborated by the relatively low effective value for the dielectric constant obtained independently An estimate of the depth of penetration of a thermal wave using the values $(k\rho c)^{-1/2}$

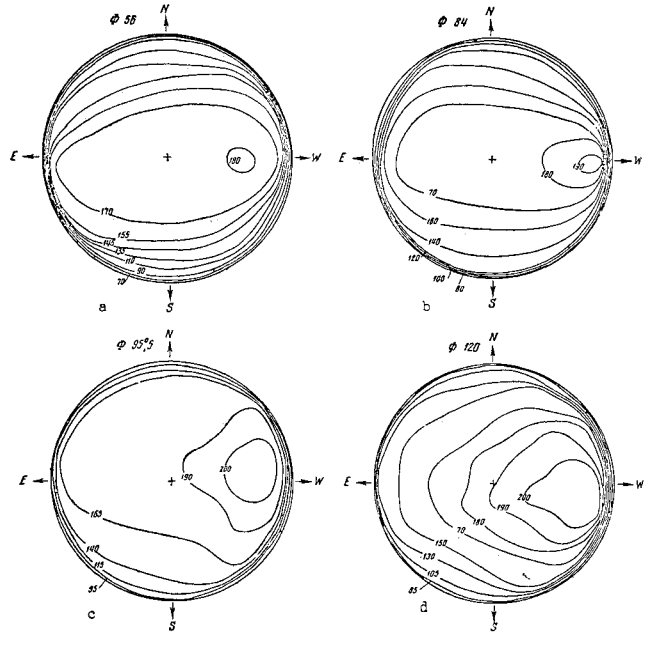

Fig 8 Radio pictures of the moon at 0 8-cm wavelength, made in 1959: a) December 4; b) December 6; c) December 7; and d) December 9 Figures on isophote lines show antenna temperature in degrees Kelvin

Table 2

λ, cm	$T\sim/T_0$	δ	δ/λ	ξ_{calc}	ξ_{obs}	c
0 8	0 19	2 0	2 5	34	30 ± 5	0 85
1 25	0 17	2 4	1 9	35	45	
1 63	0 16	2 3	1 4	35	34	
2 0	0 10	4 4	2 2	39	40 ± 5	0 40
3 2	0 075	6 1	1 9	41	45 ± 5	0 29
9 6	<0 02	>24	>2 4	44		
20 5	<0 02	>25	>1 2			

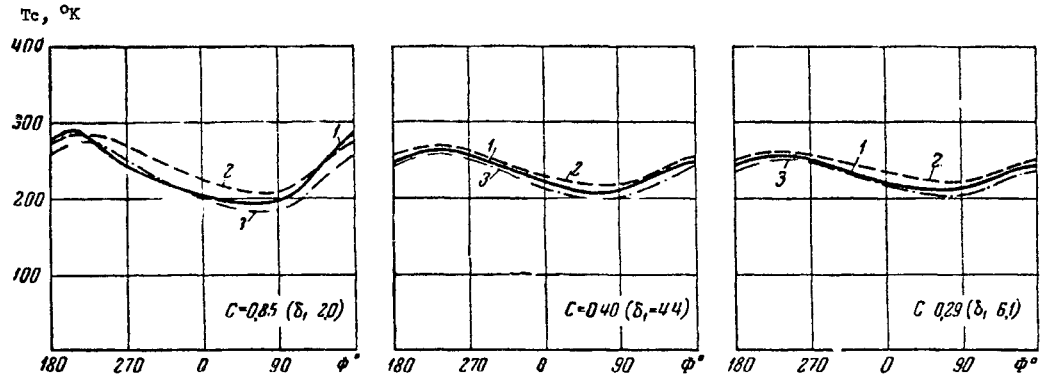

Fig 9 Phase behavior of brightness temperature of the center of the moon's disk at 0 8-, 2-, and 3 2-cm wavelength: 1) according to observations; 2) calculation with $(k\rho c)^{-1/2} = 380$; 3) calculation with $(k\rho c)^{-1/2} = 1000$

$= 600$ and $\epsilon_{ff} \simeq 1\,5$ gives an effective value for the density of the emitting layer of 0 5 g/cm^3

On these assumptions the thermal conductivity may be equal to $k = 3\,5 \times 10^{-5}$ and the depth of penetration of a thermal wave is about 20 cm Assuming that $\delta = 2\lambda$, we obtain a depth of penetration of electromagnetic waves of $\sim 40\lambda$ For example, a wave 2 cm long penetrates to a depth of about 1 m The loss angle at this wavelength is very small, $\sim 10'$

The larger value for the parameter δ for 0 8-cm wavelength apparently means that there is a gradual decrease in density and thermal conductivity in the direction of the surface

3 The Planets

Thermal radiation is one of the most important sources of information about physical conditions on the planets The flux density of the planets, like that of the moon, increases with the reduction of wavelength in accordance with the familiar relationship

$$p = 2kT_e\Omega_e/\lambda^2$$

where T is the effective radio temperature and Ω is the apparent solid angle of the planet The weak dependence of T_e on wavelength in the case of thermal radiation means that the most suitable wavelengths for observing the planets are the centimeter and millimeter wavelengths

The exceptional importance of investigating physical conditions on the planets by radio astronomy, especially when optical methods are hard to use—for example, in the case of the layer of cloud surrounding Venus and hiding its surface—means that observation of the planets is one of the most vital tasks to be assigned to the 22-radio telescope The radio astronomical studies of the planets described next are being made by A D Kuz'min and A E Salomonovich

The inadequate sensitivity of the receiving equipment used for the centimeter wavelengths has so far limited the time of observation of the planets to the periods of their closest approach to the earth

In September–November 1959 and March–July 1961 observations were made of the radiation of Venus In June 1961 the radiation of Jupiter was observed

The study of Venus was made in 1959 at 0 8-cm wavelength at a period close to the inferior conjunction of the planet,[29] using visual observations to give a slow transit of the antenna pattern across Venus on one of the coordinates (at a relative velocity of 0 5–4 min of arc per min of time) and tracking on the other The antenna temperature measurements were converted to effective averages for the disk of Venus using the values obtained for the effective area of the antenna Seventeen days after inferior conjunction it was found that $T = 315 \pm 70$°K, which, allowing for errors of measurement, does not disagree with the value of T found by Gibson and McEwan [30] There was found to be a regular increase in T as Venus moved away from inferior conjunction, when the part of the disk visible from the Earth which was lighted by the sun increased in size

Certain predictions have been made as to physical conditions on Venus Since the effective temperature of the disk at 0 8-cm wavelength increases with the growth of the lighted proportion of the disk, we can speak of a probable difference of temperature in the lighted and unlighted parts of the disk The presence of phase behavior shows that at least part of the radiation of Venus is emitted by the solid surface of the planet, and that the period of rotation of Venus around its axis cannot be too short, since if it were there would be an averaging of the brightness temperatures of the lighted and unlighted parts of the disk The significant difference in the brightness temperature at 0 8-cm wavelength from that measured by American investigators at 3 2-cm wavelength[31] can be explained by the absorption of the shorter radio waves in the relatively cold atmosphere of Venus This suggestion was developed later in Barrett's paper [32] In the presence of absorption we should expect phase behavior at 3-cm wavelength, as remarked in Ref 29 In papers published later this suggestion was confirmed [33]

During the period close to inferior conjunction in 1961, the observations of Venus were repeated They were made over a longer period of time at 0 4-, 0 8 , 3 3-, and 9 6-cm wavelengths Preliminary data[34] show that the brightness temperature T of the unlighted disk at 0 4 and 0 8 cm is close to 400°K There is an increase in T with distance from inferior conjunction

The average value of T measured at 3 3-cm wavelength between May 26 and July 10–that is, over 1 5–2 months after inferior conjunction, was found to be 542°K A tendency was noted to a regular increase in T with distance from inferior conjunction Linear extrapolation of this variation to the time of inferior conjunction gives a brightness temperature of the unlighted side of the planet close to 400°K

At 9 6-cm wavelength the average value for the period of measurement was $T = 690$°K The fluctuations in T noted in Ref 34 do not in most cases exceed the limits of chance error, although there were isolated cases of abnormally high values of T_e which could not be explained in this way

The properties noted lead to the assumption that there may be a component of radiation at decimeter wavelengths for which the ionosphere of Venus may be partly responsible

On the other hand, the relatively small difference in temperatures measured at 0 4-, 0 8-, and 3 3-cm wavelengths casts doubt on the suggestion that there is high pressure and a high water vapor content in the atmosphere of Venus [32]

It should be noted that the data on hand do not yet make it possible to give preference to any of the several theories relating the observed strength of radiation of Venus to physical conditions on its surface and in the atmosphere [32 35–37]

Further investigation of physical conditions on Venus requires long-term observation over a wide range of radio frequencies, including those near the water-vapor absorption line (13 5 mm) and at wavelengths in the decimeter range

References

[1] Karachun, A M, Kuz'min, A D, and Salomonovich, A E, Radiotekhn i Elektron (Radio Eng Electron) **VI,** 430 (1961)

[2] Karachun, A M, Kuz'min, A D, and Salomonovich, A E, Astron Zh (Astron J) **38,** 83 (1961)

[3] Kislyakov, A G, Kuz'min, A D, and Salomonovich, A E, Izv Vysshikh Vchebn Zavedenii, Radiofizika (University Bulletins, Radiophysics) **4,** 573 (1961)

[4] Westerhout, G, Bull Astr Inst Netherl **14,** 215 (1958)

[5] Apushkinskii, G P and Pariiskii, Yu N, Astron Zh (Astron J) **36,** 739 (1959)

[6] Mezger, P G, Telefunkenzeitung **124,** 99 (1959)

[7] Salomonovich, A E, Astron Zh (Astron J) **35,** 129 (1958)

[8] Kuz'min, A D, Radiotekhn i Elektron (Radio Eng Electron) **3,** 561 (1958)

[9] Mayer, C H, McCullough, T P, and Sloanaker, R M, Astrophys J **126,** 468 (1957)

[10] Esepkina, N A, Dokl Akad Nauk SSSR (Proc USSR Acad Sci) **113,** 1 (1958)

[11] Kalachev, P D and Salomonovich, A E, Tr Fiz Inst im Lebedeva (Trans Lebedev Phys Inst) **17,** 13 (1962)

[12] Kuz'min, A D and Salomonovich, A E, Astron Zh (Astron J) **39,** 660 (1962)

[13] Kuz'min, A D, Tr Fiz Inst im Lebedeva (Trans Lebedev Phys Inst) **17,** 84 (1962)

[14] Salomonovich, A E, Pariiskii, Yu N, and Khangil'din, U V, Astron Zh (Astron J) **35,** 659 (1958)

[15] Salomonovich, A E, Koshchenko, V N, and Noskova, R I, Byul Solnechnye Dannye (Solar Data Bulletin) **9,** 83 (1959)

[16] Salomonovich, A E, Astron Zh (Astron J) **37,** 969 (1960)

[17] Kaidanovskii, N L and Salomonovich, A E, Izv Vysshikh Uchebn Zavedenni, Radiofizika (University Bulletins, Radiophysics) **4,** 40 (1961)

[18] Amenitskii, N A, Noskova, R I, and Salomonovich, A E, Astron Zh (Astron J) **37,** 185 (1960)

[19] Koshchenko, V N and Salomonovich, A E, Izv Vysshikh Uchebn Zavedenii, Radiofizika (University Bulletins, Radiophysics) **4,** 591 (1961)

[20] Koshchenko, V N, Losovskii, B Ya, and Salomonovich, A E, Izv Vysshikh Uchebn Zavedenii, Radiofizika (University Bulletins, Radiophysics) **4,** 596 (1961)

[21] Koshchenko, V N, Kuz'min, A D, and Salomonovich, A E, Izv Vysshikh Uchebn Zavedenii, Radiofizika (University Bulletins, Radiophysics) **4,** 425 (1961)

[22] Troitskii, V S, Astron Zh (Astron J) **31,** 511 (1954)

[23] Piddington, J H and Minnett, H C, Australian J Sci Research 2A, 63 (1949)

[24] Zelinskaya, M R, Troitskii, V S, and Fedoseev, L I, Astron Zh (Astron J) **36,** 643 (1959)

[25] Mezger, P G and Strassl, H, Planetary Space Sci **1,** 213 (1959)

[26] Jaeger, J C, Australian J Phys **6,** 10 (1953)

[27] Salomonovich, A E, Astron Zh (Astron J) **39,** 79 (1962)

[28] Pettit, E and Nicholson, S B, Astrophys J **71,** 102 (1930)

[29] Kuz'min, A D and Salomonovich, A E, Astron Zh (Astron J) **37,** 297 (1960)

[30] Gibson, J and McEwan, R J, *Radioastronomiya, Parizhskii Simpozium* (*Paris Symposium on Radio Astronomy*) (Foreign Literature Press, 1961), p 56 [English edition: *Paris Symposium on Radio Astronomy*, edited by Bracewell (Stanford University Press, Calif, 1959), p 50—translator]

[31] Mayer, C H, McCullough, T P, and Sloanaker, R M, Astrophys J **127,** 1 (1958)

[32] Barrett, A H, Astrophys J **133,** 281 (1961)

[33] Mayer, C H, McCullough, T P, and Sloanaker, R M, Report to the Twelfth General Assembly of URSI (London, 1960)

[34] Kuz min, A D and Salomonovich, A E, Astron Zh (Astron J) **38,** 1115 (1961)

[35] Jones, D E, Planetary Space Sci **5,** 166 (1961)

[36] Sagan, C, Science **133,** 849 (1961)

[37] Öpik, E, J Geophys Res **66,** 2807 (1961)